Supporting Information

Zheng et al. 10.1073/pnas.1201240109

SI Methods

Collagen Gel Preparation. Type I collagen was extracted from rat tails under sterile conditions, lyophilized, and dissolved in 0.1% acetic acid following a standard protocol (1). A stock solution of collagen was prepared at the concentration of 15 mg/mL, which was further diluted and neutralized to 6 or 10 mg/mL with buffer solutions [1x Medium 199 (M199, Lonza), 10x M199, and 1 mol l^{-1} NaOH] on ice prior to the microvessel fabrication. For the study of endothelial-perivascular interactions, appropriate volume of concentrated suspension of perivascular cells was mixed into the neutralized collagen solution on ice for the designated concentration of collagen gels and density of cells.

Microvessel Scaffold Fabrication. The microvessel networks were fabricated within type I collagen at the concentrations of either 6 mg/mL (Fig. 3) or 10 mg/mL (Figs. 1 and 2), and housed between two plexiglass pieces, which were sealed with mechanical pressure (Fig. 1*B* and Fig. S1). Upon fabrication, both plexiglass pieces were first sterilized via exposure to oxygen plasma (Harrick, 100 W for 4 min) and coated with 1% (v/v) polyethylenimine (PEI) and 0.1% (v/v) glutaraldehyde to provide adhesion to the collagen gels. The top plexiglass (Fig. S1*A*, *6*) contained a well (20 mm × 20 mm × 1 mm) to define the thickness, size, and shape of the top collagen scaffold. There were two injection ports on the plexiglass; one was for injecting the collagen gel and the other for air to evacuate from the closed mold during the injection. Two stainless steel dowel pins were inserted into the other two holes in the top plexiglass to define inlet and outlet of the microvessel networks. The top jig was assembled (Fig. S1*A*, *1*) by making a sandwich with the PDMS stamp on the bottom (Fig. S1*A*, *4*), the aluminum piece in the middle for alignment (Fig. S1*A*, *5*), and the top plexiglass on the top. The neutralized collagen gel with or without cells was then injected into the assembled top jig through one of the injection ports with a 1-mL syringe. The bottom plexiglass (Fig. S1*A*, *7*) contained a well (25 mm × 25 mm × 0.2 mm) to define the thin flat layer of the bottom collagen. Upon fabrication, the neutralized collagen gel was dispensed on the glass coverslip in the bottom plexiglass, followed by placing a flat slab of PDMS stamp on the top (Fig. S1*A*, *2*).

The collagen gel was allowed to cross-link for 30 min at 37 °C and 5% CO_2. The assembled top jig (Fig. S1*A*, *1*) contained the collagen gel with microfluidic structure, which would become the top part of the microchannel networks, and the assembled bottom jig (Fig. S1*A*, *2*) contained a thin layer of collagen that would be the bottom of the networks. The device was assembled by placing the top plexiglass containing collagen scaffold with the microfluidic structures on the bottom plexiglass containing the flat slab of collagen gel (Fig. 1*B* and Fig. S1*A*, *3*) and sealed by mechanical pressure. A PDMS reservoir (approximately 6 mm thick) (Fig. S1*A*, *8*) was placed on the top of the device to serve as extended reservoirs over the inlet and outlet. Culture medium was added to the reservoirs and the assembled device was incubated at 37 °C and 5% CO_2 for 2 h to allow the medium to replace the PBS buffer that remained in the device from assembly before seeding cells.

Cell Seeding and Culture. Human umbilical vein endothelial cells (HUVECs) (Lonza), human brain vascular pericytes (HBVPCs) (ScienCell Research Laboratories), and human umbilical cord arterial smooth muscle cells (HUASMCs) (Lonza) at passage numbers 3 to 8 were used. HUVECs, HBVPCs, and HUASMCs were maintained in culture flasks with growth medium (GM), pericyte medium (PM), and smooth muscle cell growth media (SmGM) respectively, in 37 °C incubators with 5% CO_2 and ambient oxygen. Two types of endothelial growth media were used with one containing base medium M199 with 2% fetal bovine serum (FBS), and the other with 16% FBS. No significant differences were observed in the morphology or behavior of endothelial cells with these two different media.

Prior to seeding in collagen microchannels, HUVECs were trypsinized from the culture flask and suspended in growth media with density of 4.5×10^6 cells mL^{-1}. The growth media was removed from the reservoirs in the device with gel loading pipette tips and 10 μL of cell suspension was added to one reservoir such that the suspension flowed into the channels. The cell-seeded devices were then placed back into incubators to allow cell attachment on the inner walls of the microchannels for 20 min. The culture medium with or without vasculogenic growth factors was then placed in both reservoirs with initial height difference of around 6 mm and refreshed every 12 h. This unbalanced initial condition in the levels of medium equilibrated over a period of approximately 2 h. This procedure defined a decaying, unidirectional Poiseuille flow within the channels with an average shear stress of approximately 0.1 dyne cm^{-2}.

In microvessel scaffolds containing cocultures (ECs with either HBVPCs or HUASMCs), HBVPCs or HUASMCs were trypsinized from the culture flask and suspended in their media with density of 2.0×10^6 cells mL^{-1}. Appropriate volumes of this cell suspension were mixed well with neutralized collagen to achieve the targeted concentrations of perivascular cells (1.0×10^5 cells mL^{-1}) and of collagen (6 or 10 mg/mL).

Growth media—type I (GM): M199 with 16% FBS, L-glutamine, penicillin/streptomycin (P/S), (Lonza) and endothelial cell growth supplement (ECGS, Millipore Co.).

Growth media—type II (GM) (single quote kits from Lonza): M199 with 2% FBS, 1% P/S, epidermal growth factors (EGF), bovine brain extract with heparin (BBE), hydrocortisone, ascorbic acid, gentamicin and amphotericin B.

Proangiogenic media (VM): GM with 50 ng mL^{-1} vascular endothelial cell growth factor (VEGF), 50 ng mL^{-1} basic fibroblast growth factor (bFGF), 50 ng mL^{-1} Phorbol-12-myristate-13-acetate (TPA, Millipore Co.), and 50 ng mL^{-1} L-ascorbic acid (Acros Organics).

Pericyte media (PM) for HBVPCs: basal pericyte medium with 2% FBS, 1% pericyte growth supplement (PGS), and 1% P/S. (ScienCell Research Laboratories).

Smooth muscle cell growth media (SmGM) for HUASMCs: smooth Muscle Cell Basal Medium with 5% FBS, insulin, hFGF-2, gentamicin, hEGF, and 1% P/S (Lonza).

Immunofluorecence Stainings. At the designated time point, the devices were fixed in situ with 3.7% formaldehyde, washed three times with PBS, and immunohistochemically stained for CD31, α-Smooth muscle actin, and desmin; all reagents were delivered through the microchannels. The devices were first incubated for 30 min in a blocking solution consisting of 2% bovine serum albumin and 0.5% Triton-X for membrane permeablization. The devices were then incubated with primary antibodies overnight and secondary antibodies for 2 h. CD31 immunohistochemistry was performed using a rabbit polyclonal antibody CD31/platelet endothelial cell adhesion molecule-1 (1:50 dilution, Abcam). α-Smooth muscle actin immunohistochemistry was performed using a mouse monoclonal α-SMA (1:100 dilution, Invitrogen

Co.). Desmin immunohistochemistry was performed using a mouse monoclonal desmin (1:100 dilution, Invitrogen Co.). In addition, nuclei were stained with DAPI (Invitrogen Co.) for both cell identification and counting.

Analysis of Microfluidic Vascular Networks (μVNs). The immunofluorescence images of μVNs were taken in situ using a Zeiss 510 Meta or a Nikon A1R confocal microscope. Image stacks were accumulated with a z-step between each successful optical slice of approximately 2 μm. Cross sections and three-dimensional (3D) reconstructions were generated from z-stacks of images in ImageJ with orthogonal projection, z-projection and 3D viewer. The density and length of endothelial sprouts from the microvascular network were measured in z-stacks of confocal images. In addition, for the co-culture experiment, perivascular recruitment around the vessel was analyzed through the expression of α-SMA and desmin. A 20-μm-thick zone around the vessels was defined for quantification of coating ratio; the fraction of positive-stained perivascular cells was counted in ImageJ. With the original seeding density of ECs (200–400 cells mm^{-2} in the lumen) and perivascular cells (0.1×10^6 cells mL^{-1} in the collagen bulk), we estimated that the original cell ratio of perivascular cells around the vascular network (PC:EC) was 0.05:1.

Ultrastructral Analysis. All reagents were purchased from Electron Microscopy Sciences. For scanning electron microscopy (SEM), μVNs were fixed, dehydrated, critical-point-dried, sputter-coated with platinum-palladium, and analyzed using a FEI Sirion scanning electron microscope with an accelerating voltage of 5 kV. For transmission electron microscopy, constructs were perfused with modified Karnovsky's fixative (2.5% glutaraldehyde, 4% paraformaldehyde, 0.02% picric acid in 0.1 M sodium cacodylate buffer, pH 7.3) overnight. Blocks (1 mm^3) were postfixed in 1% osmium tetroxide/1.5% potassium-ferricyanide, stained with 1.5% uranyl acetate, and dehydrated through graded ethanol series. After embedding in Spurr's resin, sections were cut at 55–60 nm thickness using a Diatome diamond knife on a Leica Ultracut S ultramicrotome. Sections were contrasted with lead citrate and viewed on a JEOL JEM 100 CX-II electron microscope operated at 80 kV. Images were recorded on Kodak 4489 Electron Image film and then digitized at 900 dpi for publication.

Live Imaging of Whole Blood Perfusion and VWF Secretion. Fresh blood was drawn into 3.8% (0.129 M) sodium citrate from consenting healthy donors under protocols approved by the Institutional Review Board of the University of Washington. The blood was then centrifuged at 120 g for 15 min to isolate the platelet-rich plasma and buffy coat. Platelets in the plate-rich plasma were labeled with Percp-cy5.5 conjugated CD41a antibody (1 μg mL^{-1}) for 20 min at room temperature, and leucocytes in the buffy coat were labeled with FITC-conjugated CD45 antibody. The labeled platelets and leukocytes were reconstituted with red blood cells at the original ratio into whole blood.

The whole blood perfusion experiments were carried out in the μVNs after culturing them in growth media for 7 to 14 days; no differences were detected in the behavior of the vessels within this time range. The growth medium in the endothelial lumens was first washed away with PBS, followed by the blood perfusion through the μVNs at shear stresses between 10 and 30 dyne cm^{-2} for 15 min to one hour. The vessels were monitored through bright field and fluorescence imaging using an inverted microscope (Olympus, IX81). The fluorescence arising from individual platelets and aggregates attached to the vessel wall was recorded with a digital camera (CoolSNAP—at 1–5 fps), and analyzed using SlideBook. Platelet adhesion was quantified using Matlab for control and stimulated vessels with four replicates at each condition. After each experiment, the microvessel network was washed with PBS immediately, then fixed and stained for an endothelial marker (CD31) for further imaging.

Studies of VWF secretion and the interactions of blood with stimulated μVNs were performed as follows: The μVNs were activated with PMA (50 ng mL^{-1} in growth media) for 20 min at 1 μL min^{-1} (shear stress approximately 1 dyne cm^{-2}), then washed with PBS buffer before perfusion of a FITC-conjugated VWF antibody (Abcam—100 μg mL^{-1} in growth media), or whole blood with labeled platelets. Live imaging was performed through a fluorescence microscope, and 3D structures were imaged and obtained in situ through a confocal microscope.

Measurement of Endothelial Permeability. We measured the diffusivity of small and large molecules in the acellular collagen matrix by delivering solutions of fluorescein (Sigma-Aldrich—10 μmol L^{-1} in PBS) and 70 kDa FITC—Dextran (Sigma-Aldrich—10 μmol L^{-1} in PBS) into the scaffold via microchannels (flow rate of 10 μL min^{-1}). As soon as the microchannels were filled, the delivery was stopped and fluorescence images were acquired sequentially for 3–30 min with an inverted microscope (Olympus, IX81) using a CCD camera (Hamamatsu, Orca-ER). The images were analyzed using Slidebook software (Olympus) to estimate the diffusivity of fluorescent molecules in the collagen gels, as described previously (2).

To determine the permeability of the endothelium, transient delivery experiments were carried out in μVNs (Figs. 1*E* and 2 *A–C* and Fig. S4). Fluorescent solutions in PBS were delivered through the channels with live endothelium at a continuous flow rate of 2 μL min^{-1}. Fluorescence images were acquired sequentially and image analysis was carried out in MATLAB (The Mathworks) to estimate the permeability of the endotheliaum, K [cm s^{-1}] as a function of known parameters (intensity of fluorescent solution, i_0, initial background intensity i_{initial}, intensity at the interchannel center i_c, diffusivity of solute in collagen, D_{collagen}, interchannel distance δ, and time t) based on the model of mass transfer developed below. Average values for K were obtained from four K values derived in each five-channel device, and three to six devices were used for each condition (Fig. S3 *B* and *C*).

We present the analysis of data such as in Fig. 1*E*. Fig. S3 illustrates our analysis of the transient diffusion of a solute from microchannels into the bulk material. In our analysis, we make two assumptions: The fluorescence intensity is proportional to the concentration of the fluorescent solute; this assumption is good for low concentration ranges of fluorescence (3) (1–10 μM fluorescence labeled solutes were employed in this presentation); and the concentration within the solution in the microchannels remains constant with respect to both time and the axial position along the channels; these approximations are accurate because we maintained sufficiently high flow rate to ensure high Péclet number ($Pe \sim 10^5$) within the flow and high Biot number ($Bi \sim 10^3$) for mass transfer from the solution to the walls of the channel (2). The uniformity along the axial direction allows for the study of temporal modulation of fluorescence intensity within the bulk materials in a spatially uniform manner.

We take the constant fluorescent intensity within the channel to be i_0 (Fig. S3*B*) and the intensity profile within the interchannel space (i.e., collagen bulk) to be $i(x, t)$. The solutes have diffusivity in collagen (D_{collagen}[m^2 s^{-1}]), and permeability coefficient across the endothelium at the microchannel boundary (K [m s^{-1}]). We nondimensionalize the parameters as follows: The axis orthogonal to five vertical channels, as shown in Fig. S3*B* is defined as $X = x/(\delta/2)$, the fluorescence intensity defined as $I(X, \tau) = \frac{i(x,t)-i_0}{i_{\text{initial}}-i_0}$, and the time is defined as $\tau = \frac{D_{\text{dye/collagen}}t}{(\delta/2)^2}$ (the Fourier modulus).

In the region of interchannel collagen bulk, the governing equations for concentration distribution of solutes in scaled form is

$$\frac{\partial^2 C}{\partial X^2} = \frac{\partial C}{\partial \tau} \qquad \textbf{[S1]}$$

The initial condition on Eq. **S1** is $C(X,0) = 1$. The boundary conditions on Eq. **S1** are: No flux at the center of interchannel space ($X = 0$), and continuity of flux at the boundaries with the microchannels ($X = 1$):

$$\frac{\partial C(0,\tau)}{\partial X} = 0, \qquad \frac{\partial C(1,\tau)}{\partial X} = -BiC(1,\tau) \qquad \textbf{[S2]}$$

where the Biot number is defined as

$$Bi \equiv \frac{K\delta/2}{D_{\text{collagen}}} \qquad \textbf{[S3]}$$

With these conditions, Eq. **S1** has the following solution:

$$C = \sum_{n=1}^{\infty} A_n e^{-\lambda_n^2 \tau} \cos(\lambda_n X), A_n = \frac{4\sin\lambda_n}{2\lambda_n + \sin(2\lambda_n)}, \qquad \textbf{[S4]}$$

where λ_n is given by

$$\lambda_n \tan\lambda_n = Bi. \qquad \textbf{[S5]}$$

For $\tau > 0.2$(i.e. $t > 23$ s for 332 kDa fluorescein or $t > 5$ min for 70 kDa FITC-Dextran), the above solution reduces to:

$$C = \frac{4\sin\lambda_1}{2\lambda_1 + \sin(2\lambda_1)} e^{-\lambda_1^2 \tau} \cos(\lambda_1 X), \qquad \textbf{[S6]}$$

At the center of interchannel space, we can further simplify the solution to be:

$$C_c = C(X=0,\tau) = \frac{i_c - i_0}{i_{\text{initial}} - i_0} = \frac{4\sin\lambda_1}{2\lambda_1 + \sin(2\lambda_1)} e^{-\lambda_1^2 \tau}. \qquad \textbf{[S7]}$$

Taking the logarithm of both sides of Eq. **S6** and moving back to dimensional variables, we have:

$$\ln\frac{i_c - i_0}{i_{\text{initial}} - i_0} = -\lambda_1^2 \frac{D_{\text{collagen}} t}{(\delta/2)^2} + \ln\frac{4\sin\lambda_1}{2\lambda_1 + \sin(2\lambda_1)}. \qquad \textbf{[S8]}$$

Thus, a linear fit of $\ln\frac{i_c - i_0}{i_{\text{initial}} - i_0}$ vs. t gives λ_1 and via Eq. **S4**, **S5** and the definition of Bi (Eq. **S3**) we obtain the permeability of the μVNs:

$$K = \frac{D_{\text{collagen}}}{\delta/2} \lambda_1 \tan\lambda_1. \qquad \textbf{[S9]}$$

Statistical Analysis. Independent or paired t tests were used to compare group means for data presented in Figs. 2*D* and 3*C*. A p value <0.05 was considered significant for all tests. Three to six independent experiments were performed for each condition tested unless otherwise stated. In all bar plots, the data is presented as mean ± standard error from three to six samples for each experimental condition.

1. Cross VL, et al. (2010) Dense collagen matrices with microstructure and cellular remodeling for 3D cell culture. *Biomaterials* 31:8596–8607.
2. Choi NW, et al. (2007) Microfluidic scaffolds for tissue engineering. *Nat Mater* 6:908–915.
3. Sharma A, Schulman SG (1999) *Introduction to Fluorescence Spectroscopy* (Wiley-Interscience, New York) p 173.

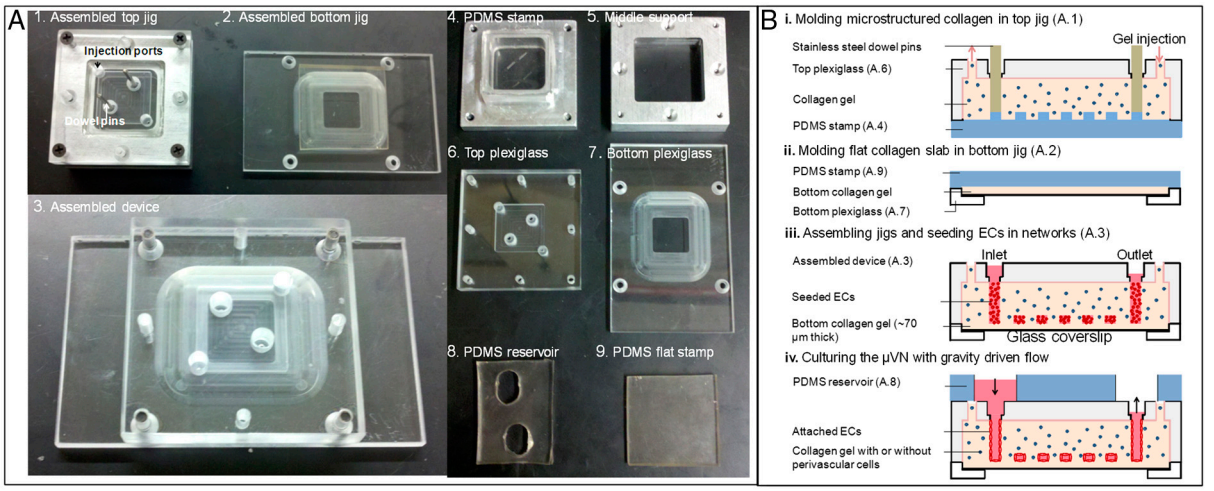

Fig. S1. Parts and schematics for microvessel fabrication in type I collagen (Fig. 1*B*). (*A*) (*1*) Assembled top jig to define microstructures and fluid connection ports. Steel dowel pins used to block exit of collagen through ports during injection are shown. (*2*) Assembled bottom jig to define bottom thin collagen. (*3*) Assembled device with enclosed collagen microstructures between inlet and outlet reservoirs. (*4*) PDMS stamp molded from lithographically defined SU-8 microstructures. (*5*) Middle layer aluminum piece to support PDMS stamp and alignment with top plexiglass piece. (*6*) Top plexiglass piece for the microstructured collagen. (*7*) Bottom plexiglass piece with glass coverslip. (*8*) Additional reservoirs for sustained gravity-driven flow through the vessels. (*9*) PDMS flat stamp to define bottom slab of collagen on glass coverslip. (*B*) Schematics of fabrication procedures: (*i*) molding the microstructured collagen in top jig; (*ii*) molding flab collagen slab in bottom jig; (*iii*) assembling the jigs mechanically and seeding cells through the inlet and outlet reservoirs; and (*iv*) culturing the microvessel network with gravity driven flow.

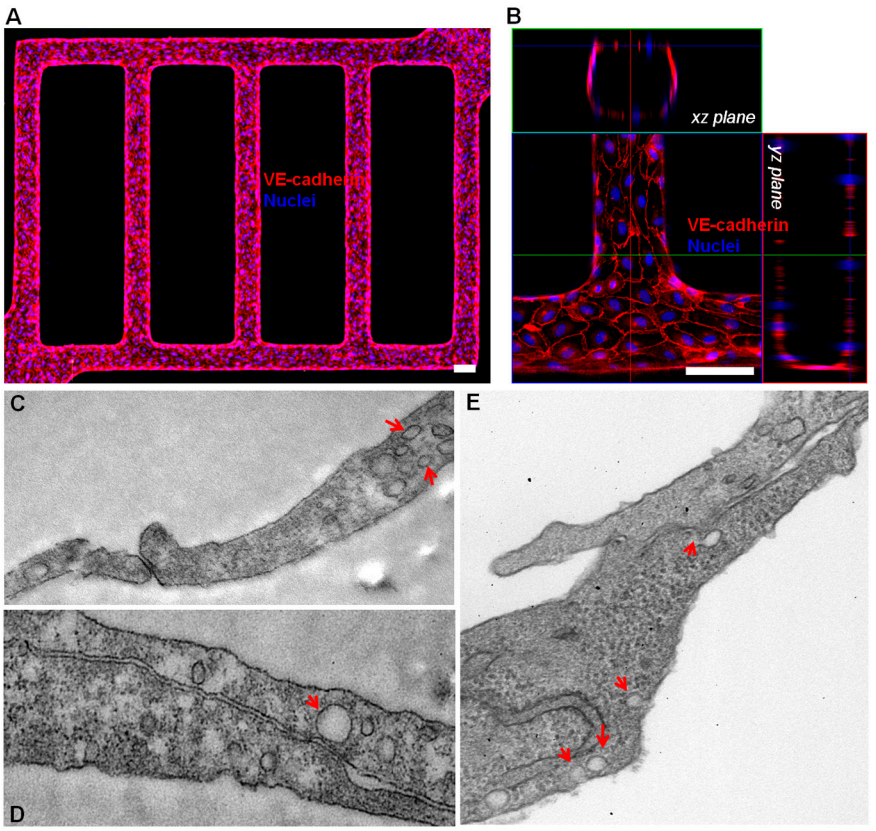

Fig. S2. Microfluidic vessel networks (μVNs) (Fig. 1 *C* and *D*). (*A* and *B*) Z-projection of confocal sections of endothelialized microvessel network (overall network, *A*, and zoomed views, *B*). Red, VE-Cadherin; blue, nuclei. (Scale bar: 100 μm.) (*C*–*E*) Electron micrographs of endothelial junctions and intracellular vesicles (focal contacts, *C*; overlapping junctions, *D* and *E*). Arrows, Pinocytotic vesicles. (Magnification: 29,000×.)

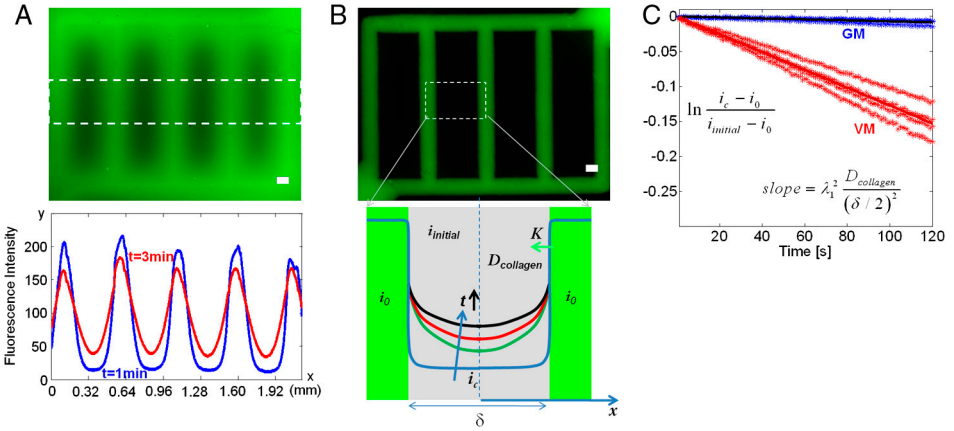

Fig. S3. Delivery of solutes (70 kDa FITC-Dextran) through acellular network (*A*) and endothelialized network (*B* and *C*) in 10 mg/mL collagen. (*A*) (*Upper*) Fluorescence micrographs of nonendothelialized microfluidic in 10 mg/mL collagen network after 3 min delivery of 70 kDa FITC-Dextran via microchannels. Dash blocks are selected at the center of network to extract averaged intensity profile along *y* axis). (*Lower*) Profiles of fluorescence intensity across microvessels at two different time points. (Scale bar: 100 μm.) (*B*) (*Upper*) Example fluorescence micrograph in of μVNs, as in Fig. 1*E*. (*Lower*) Schematic diagram of the time evolution of mass transfer from solutions in a section of the microfluidic scaffold as solute passed from the microchannels (green) to the collagen bulk (gray) across an endothelial barrier. The parameters are as follows: i_0 is the fluorescence intensity in the channels; $i_{initial}$ is the initial fluorescence intensity as a function of x;i_c is the intensity at the center ($x = 0$); $D_{collagen}$ is the diffusivity in collagen for the fluorescent solute;K is the permeability coefficient of the endothelium covering the walls of the channels; and t is the time interval since perfusion with the fluorescent solutions was initiated. (*C*) Log-linear plot of the measured time evolution of the fluorescence intensity at the center of four interchannel spaces for two example microvessel networks, one cultured in growth media (GM, Fig. 1*E*), shown as blue lines, and the other cultured with one week of proangiogenic media (VM, Fig. 2*A*), shown as the red lines.

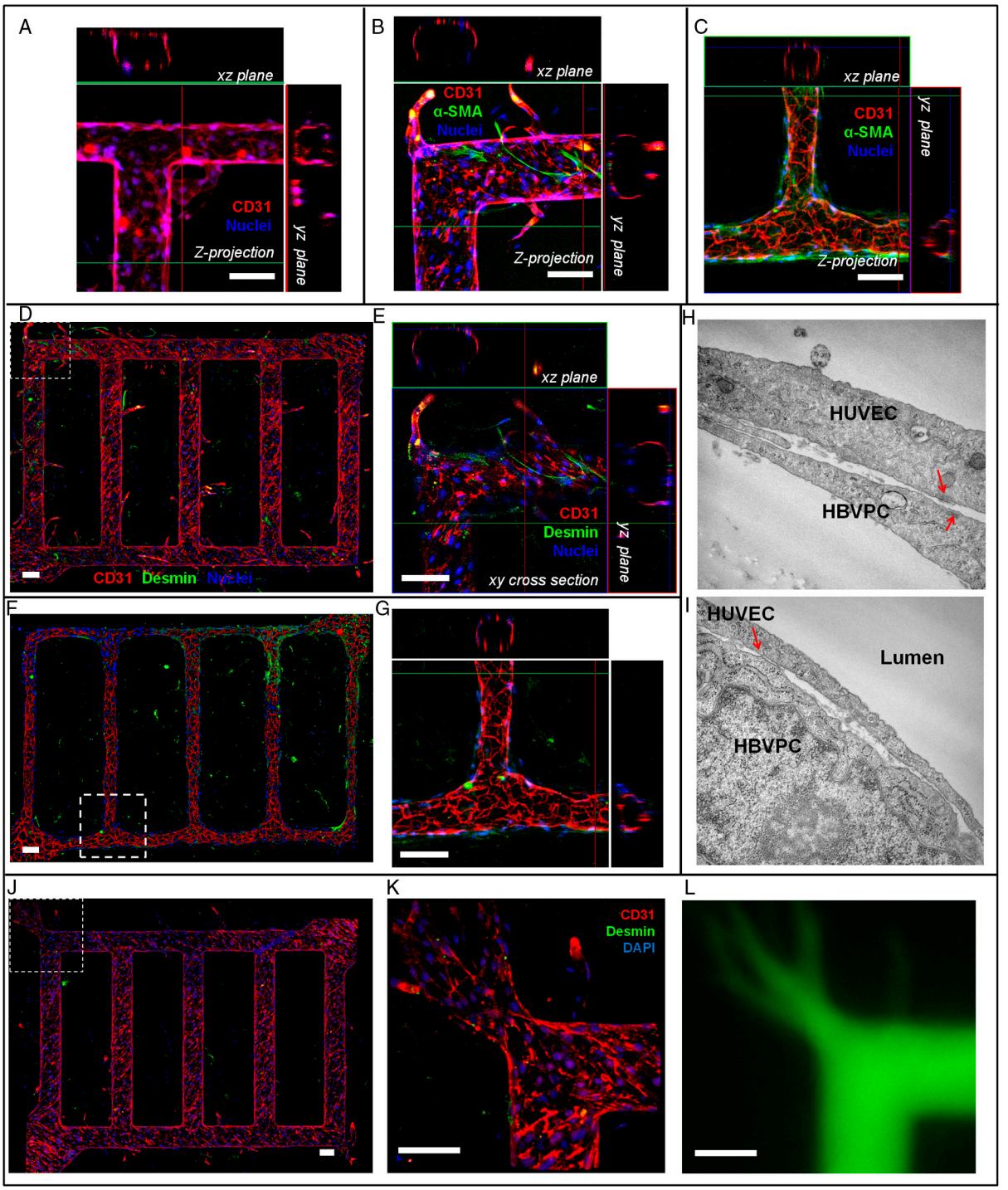

Fig. S4. Endothelial-pericyte interactions in μVNs (Fig. 2). (*A–C*) Zoomed images of (*A*) sprouting angiogenesis (Fig. 2*A*), and perivascular interactions with (*B*) endothelial sprouting (Fig. 2*B*) and (*C*) endothelial retraction (Fig. 2*C*). Red, CD31; green, α-SMA; and blue, nuclei. (Scale bar: 100 μm.) (*D–G*) Perivascular recruitment from the collagen bulk toward endothelium, with endothelial sprouting (*D*, *E*) and endothelial retraction (*F*, *G*). (*D*, *F*) The z projection of confocal sections, and (*E*, *G*) zoomed in cross-sectional views of perivascular association around the endothelium. Red, CD31; green, desmin; and blue, nuclei. (Scale bar: 100 μm.) (*H*, *I*) Electron micrographs of endothelial-pericyte interactions. (*H*) A layer of basal lamina deposited between ECs and pericytes. Arrow, Polarized focal adhesion of EC (upper cell) and pericyte (lower cell). (*I*) A pericyte located adjacent to an EC, with a layer of basal lamina between them. Arrow, Possible junction between EC and pericyte. (Magnification: 29,000×.) (*J–L*) Perivascular association around endothelium with proangiogenic stimulation. (*J*) The z-projection of confocal sections of μVNs in 10 mg/mL collagen seeded with human brain vascular pericytes, cultured in normal growth media condition for the first 7 d and proangiogenic media condition (VEGF + FGF + PMA) for the second 7 d. Red, CD31; green, desmin; and blue, nuclei. (*K*) Confocal section of corner region of interest outlined in *J*. (*L*) Snapshot image for region in *K* with delivery of 70 kDa FITC-Dextran after 1 min of perfusion at 1 μL/min. (Scale bar: 100 μm.)

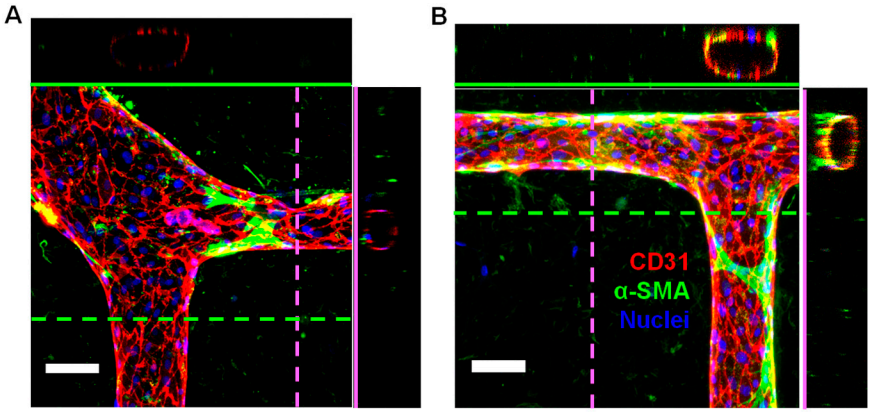

Fig. S5. Endothelial retraction with smooth muscle cell association in μVNs (Fig. 2*C*). (*A*) Endothelial retraction with buckling through the adjacent human umbilical arterial smooth muscle cells. (*B*) Endothelial retraction through the wrapping of smooth muscle cells. Red, CD31; green, α-SMA; and blue, nuclei. (Scale bar: 100 μm.)

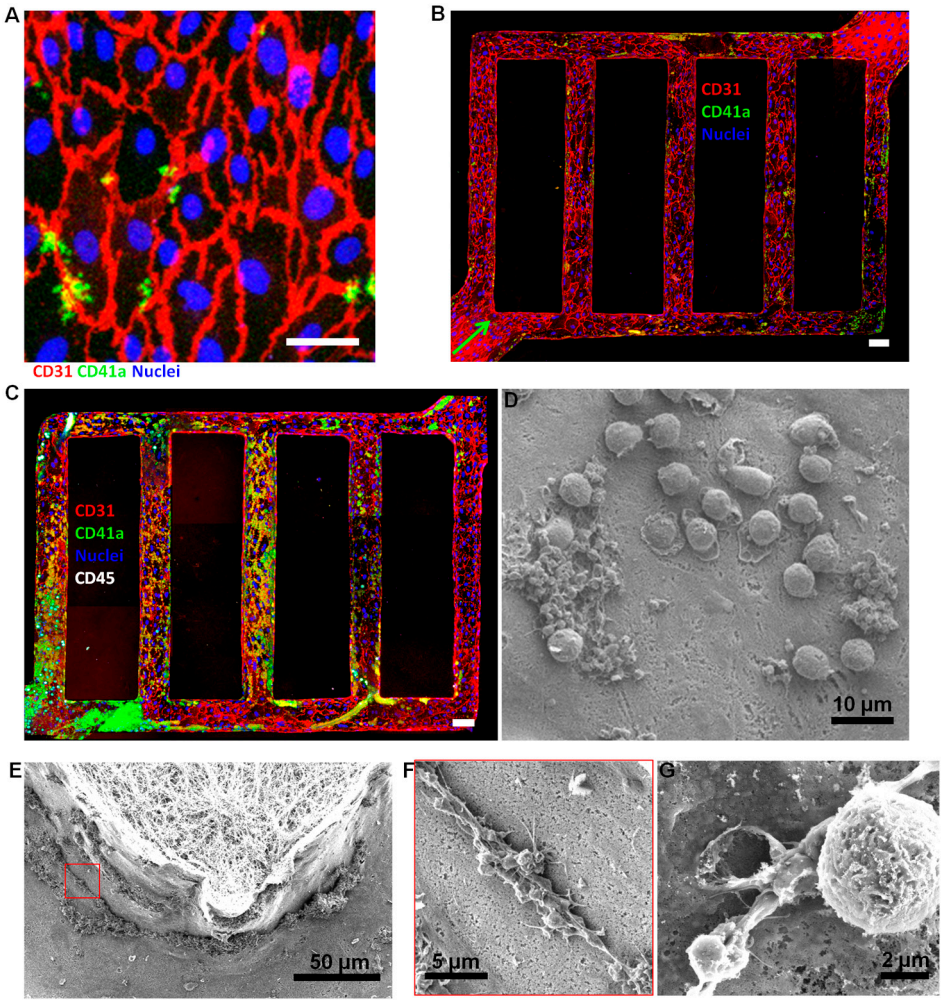

Fig. S6. Blood-endothelium interaction (Fig. 3). (*A–B*) Platelet adhesion on endothelial junctions of quiescent μVNs after 15 min of whole blood perfusion (*A*) zoomed view. (Scale bar: 50 μm.) (*B*) z projection of confocal sections of μVNs. (Scale bar: 100 μm.) Red, CD31; green, CD41a; and blue, nuclei. (*C*) Adhesion of platelets and leukocytes on stimulated μVNs after 1 h of whole blood perfusion. Red, CD31; green, CD41a; white, CD45; and blue, nuclei. (Scale bar: 100 μm.) (*D*) Scanning electron micrographs (SEM) of leukocyte adhesion on and migration through stimulated μVNs after 1 h of whole blood perfusion. (*E–G*) SEM images of (*E*) platelets strings at bifurcations (flow toward bifurcation from the bottom), (*F*) zoomed platelet strings (red box in *E*), and (*G*) zoomed images of leukocyte adhesion on platelets and endothelial membrane.

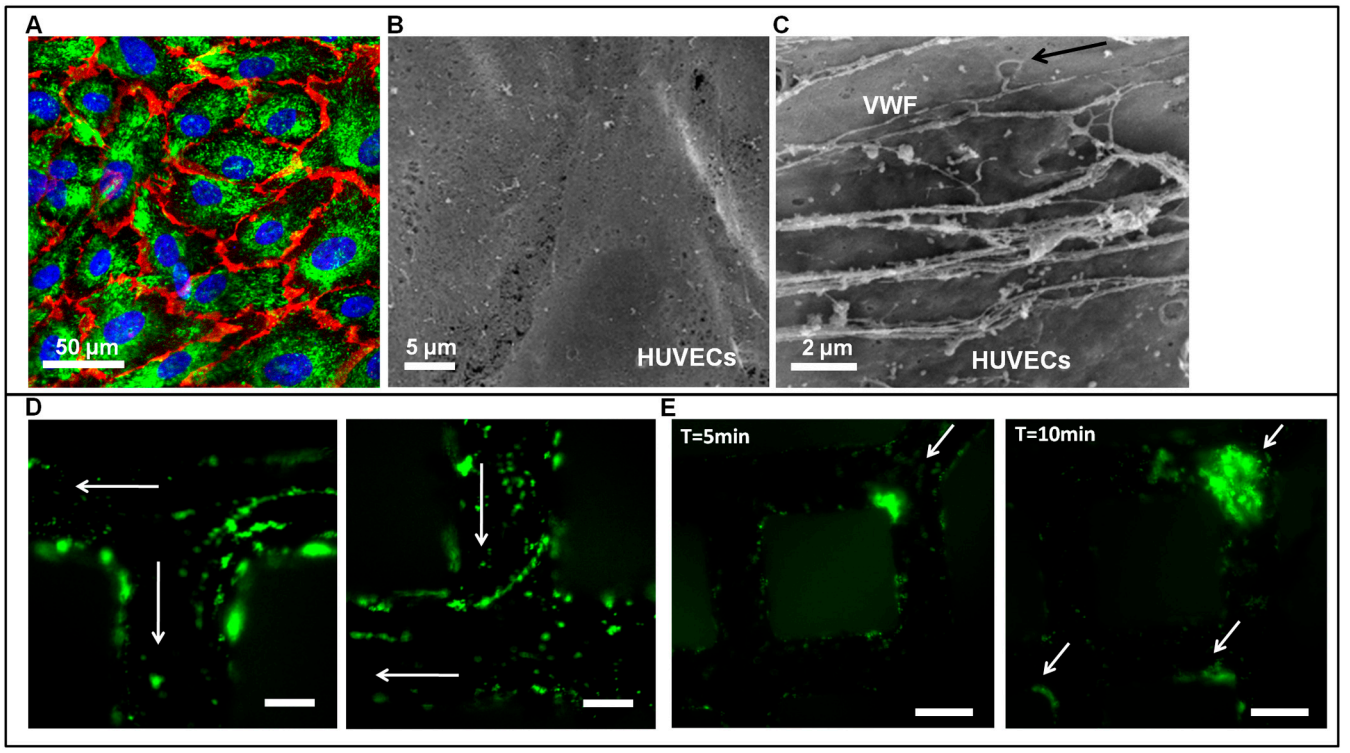

Fig. S7. VWF expression of microvascular endothelium (*A*–*C*) and spatial distribution of thrombi in uVNs (*D* and *E*) (Fig. 3 *E*–*G*). (*A*) VWF within endothelial cells in quiescent μVNs. Red, CD31; green, VWF; and blue, nuclei. (*B*) Scanning electron microscopic (SEM) image of endothelium in a quiescent μVNs. (*C*) SEM image of VWF secreted from endothelial cells of μVNs following activation by PMA. (*D*) Three-dimensional flow phenomena of platelet aggregations near flow junctions. (Scale bar: 50 μm.) (*E*) Thrombi formation at vessel bifurcation, where flow stagnation points are. (Scale bar: 100 μm.) Arrows, Flow direction. Green, platelets.

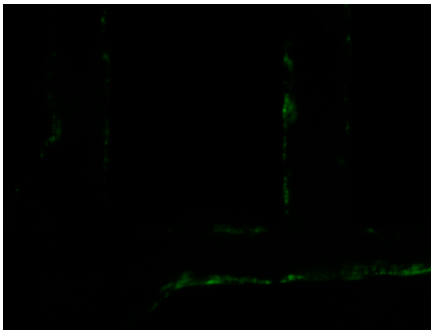

Movie S1. (Fig. 3 *A* and *B*) Whole blood perfusion (in 3.8% citrate) through a quiescent μVN. Green, CD41a.

Movie S1 (WMV)

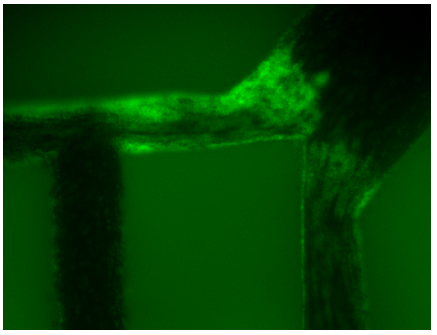

Movie S2. Whole blood perfusion (in 3.8% citrate) through a collagen microchannel network. Green, CD41a.

Movie S2 (WMV)

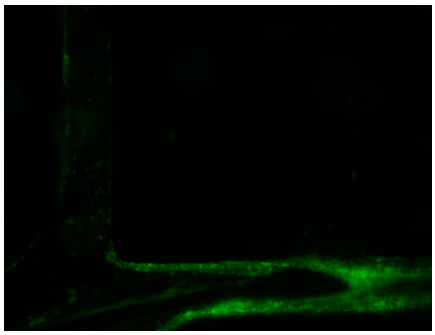

Movie S3. (Fig. 3 *A* and *B*) Whole blood perfusion (in 3.8% citrate) through a PMA stimulated μVN. Green, CD41a.

Movie S3 (WMV)